Controlling specific growth rate for recombinant protein production by *Pichia pastoris* under oxidation stress in fed-batch fermentation

Rongkang Hu
South China University of Technology
Ruiguo Cui
South China University of Technology
Qingqing Xu
South China University of Technology
Dongming Lan
South China University of Technology
Yonghua Wang (yonghw@scut.edu.cn)
South China University of Technology https://orcid.org/0000-0002-8790-4357

Research

Keywords: High cell density fermentation, Reactive oxygen species, Oxidative damage, Cell viability, Glutathione

Posted Date: July 13th, 2021

DOI: https://doi.org/10.21203/rs.3.rs-85999/v3

Abstract

Methanol can be used by *Pichia pastoris* as the sole carbon source and inducer to produce recombinant proteins in high-cell-density fermentations, but also damages cells due to reactive oxygen species (ROS) accumulation from methanol oxidation. Here, we study the relationship between methanol feeding and ROS accumulation by controlling specific growth rate during the induction phase. A higher specific growth rate increased the level of ROS accumulation caused by methanol oxidation. While the cell growth rate was proportional to specific growth rate, but maximum total protein production and highest enzyme activity were achieved at a specific growth rate of 0.05 1/h as compared to that 0.065 1/h. Moreover, oxidative damage induced by over-accumulation of ROS in *P. pastoris* during the methanol induction phase caused cell death and reduced protein expression ability. ROS scavenging system analysis reveals that the higher specific growth rate, especially 0.065 1/h, resulted in increased intracellular catalase activity and decreased glutathione content significantly. Finally, Spearman's correlation analysis further reveals that the reduced glutathione might be beneficial for maintaining cell viability and increasing protein production under oxidative stress caused by ROS toxic accumulation. Our findings suggest an integrated strategy to control the feeding of the essential substrate based on analyzing its response to oxidative stress caused by ROS toxic accumulation, as well as develop a strategy to optimize fed-batch fermentation.

Introduction

Methylotrophic yeast *Pichia pastoris* is one of the most extensively used expression systems for heterologous protein production, such as human growth hormone and lipase [1-3]. Methanol serves both as a carbon source for yeast growth in high-cell-density fermentation of *P. pastoris* and an inducer to produce heterologous proteins [4, 5]. High methanol levels lead to the accumulation of intracellular toxic oxidative by-products such as formaldehyde and peroxide to cause cell death, whereas low methanol levels reduce protein productivity by triggering proteolytic degradation of the recombinant protein [6, 7]. Therefore, methanol concentration must be carefully controlled at an adequate range to achieve the best synergy between methanol consumption and cell growth [8-10]. To control methanol within an adequate range in fed-batch fermentation, methanol feeding is the only parameter to optimize. For this purpose, the prerequisite is to understand how methanol concentration affects cell growth and protein production [11, 12].

The shift from growth solely on glycerol to growth and heterologous protein production on methanol has a drastic impact on yeast. Accumulation of reactive oxygen species (ROS) in cells caused by rapid changes in internal and external conditions can form oxidative damage [13, 14]. Methanol provides a carbon skeleton for cell growth and target protein synthesis. But methanol entering in *P. pastoris* cell will be oxidized to formaldehyde in the peroxisome molecule and produces H_2O_2. H_2O_2 is known as ROS. Increasing the methanol consumption blindly may cause the accumulation of ROS and reduce methanol utilization. Therefore, during the fermentation of *P. pastoris*, the accumulation of metabolic by-

product (H_2O_2), methanol oxidation may cause oxidative damage to cells and degradation of heterologous proteins.

The stress response of cells to environmental stress is a basic regulation mode of microbial life activities. Feeding strategies regulate cell growth and heterologous proteins by affecting cell metabolism. Methanol feed rate is relatively high in the high-density fermentation of *P. pastoris*. Similar to all other organisms, yeast cells have limited tolerance against oxidation stress, for example by enzymatic and non-enzymatic systems to respond to ROS [15]. Methanol fed-batch results in higher stress levels of organelles for protein processing [16]. The unfolded protein response-regulated oxidative folding mechanism in the endoplasmic reticulum further leads to the accumulation of intracellular ROS [17]. Therefore, the methanol feeding strategy optimized by the parameters will be limited by the methanol-induced intracellular biological response network [18]. Exploration of future optimal induction modes from cell physiological and metabolic functions is the guarantee for large-scale production of heterologous proteins.

Our study focused on the effects of specific growth rate on post-induction *P. pastoris* growth and ROS scavenging systems in high cell density fermentation. We identified the correlation of fermentation conditions with ROS-associated parameters. Then we investigated the expressions profile of genes involved in the ROS scavenging system at the mRNA level. Our findings suggest an integrated strategy to control the feeding of the essential substrate based on analyzing its response to oxidative stress caused by ROS toxic accumulation.

Materials And Methods

Strain and chemicals

P. pastoris X-33 (Invitrogen, Carlsbad, CA) strain expressing lipase (named MAS1) gene from marine *Streptomyces* sp. strain W007 was used in our study [19, 20]. Yeast extract peptone dextrose (YPD) medium for seed culture contained (g/L) yeast extract 10.0, peptone 20.0 and glucose 20.0. The basal salt medium (BSM) for batch fermentation contained (g/L) glycerol 40, 85% H_3PO_4 26.7 mL, $CaSO_4$ 0.93, K_2SO_4 18.2, $MgSO_4 \cdot 7H_2O$ 14.9, KOH 4.13, PTM1 salt solution 4.35 mL, pH 5.0. PTM1 salt solution contained (g/L) $CuSO_4 \cdot 5H_2O$ 6, NaI 0.08, $MnSO_4 \cdot 4H_2O$ 3, $ZnSO_4 \cdot 7H_2O$ 20, $FeSO_4 \cdot 7H_20$ 65, $CoCl_2 \cdot 6H_2O$ 0.5, boric acid 0.02, H_2SO_4 5mL. All other chemicals of analytical grade were supplied from Sinopharm Chemical Reagent Co., Ltd (Shanghai, China) unless otherwise indicated.

Fed-batch fermentation of lipase MAS1

The first inoculum culture was prepared from one colony of *P. pastoris* suspended in 50 mL sterilized YPD broth containing 100 μg/mL zeocin (Invitrogen, Carlsbad, CA). The culture was incubated at 30 °C in a 500-mL baffled shake-flask on rotary shaker at 250 rpm. After the OD_{600} reaches 6 in 18-24 h, a second inoculum culture was prepared by transferring the first inoculum 10% (v/v) into a 2 L baffled

shake-flask containing 400 mL sterilized YPD medium. The second inoculum culture was then incubated under the same condition as the first inoculum culture for 12 h.

The BSM (3 L) was inoculated with 10% (v/v) second inoculum into a 5-L bioreactor (BIOTECH-5BG, Baoxing Co., Shanghai, China). The initial OD_{600} of the culture in bioreactor was about 0.5. A four-phase fermentation protocol (glycerol batch, glycerol fed-batch, starvation period and constant-rate methanol feeding) was used. The bioreactor was operated at 30 °C and pH around 6.0 via adding 28% v/v ammonia. Dissolved O_2 cascade was constantly maintained above 30% air saturation. The glycerol or methanol feeding to the bioreactor was controlled by a pump. Once glycerol was depleted from culture broth, indicated by a sharp increase in DO, the glycerol fed-batch phase was started at a constant flow rate of 18 mL/(L•h) with 50% (v/v) glycerol containing 12 mL/L PTM1 solution until the biomass reached about 180 g/L (wet cell weight). After 1 h starvation period following the above high cell density fermentation, the culture was supplied with 100% (v/v) methanol containing 12 mL/L PTM1 solution to induce lipase expression corresponding to different designed specific growth rates (0.015, 0.035, 0.05 and 0.065 1/h). We ran the fed-batch fermentation employing a methanol sensor (MC-168, PTI, USA) to control methanol feeding to maintain the methanol level at 2-4 g/L. A proportional, integral and derivative control mode was applied for the methanol control system. Samples were taken at regular intervals.

Biomass, protein concentration, lipase activity and SDS-PAGE analysis

Wet cell weight (WCW) of the cell suspension was determined by centrifugation of 10 mL cell broth in a pre-weighed centrifuge tube at 8000 × *g* at 4 °C for 10 min, and the fermentation supernatant was collected and used for subsequent experiments. Total protein concentration in the supernatant was determined by the Bradford assay [21]. After lipase activity was measured using the alkali titration method [22], the obtained fermentation supernatant was analyzed by SDS-PAGE. Olive oil (Macklin, Shanghai, China) was emulsified with 4% (w/v) polyvinyl alcohol at the ratio of 1:3 (v/v). Each reaction contained 4 mL of emulsified olive oil, 5 mL of phosphate buffer at 50 mM and pH 6.0 and 1 mL of enzyme solution, and was carried out at 65 °C. The reaction was terminated by adding 15 mL of 95% (v/v) ethanol. The released fatty acids were neutralized by 0.05 M NaOH. One unit of lipase activity is defined as the amount of enzyme releasing 1 μmol of fatty acid per minute.

Cell viability and cell death

The cell viability was measured using the methylene blue dye exclusion technique [23]. The fresh fermentation broth was diluted and mixed with 0.1% (w/v) methylene blue in equal volume. After standing at room temperature for 10 min, the cells were observed under a microscope (MLS1, Mshot, China) through hemocytometer. To determine the effect of specific growth rate on cell death, cells were collected at the end of fermentation from each run, washed with PBS buffer (100 mM, pH6) and suspended in the same buffer (10^6 cells). Cell death was determined by propidium iodide staining kit (Sangon, Shanghai, China) with a fluorescence microscope (LSM800, ZEISS, Jena, Germany).

Cellular ROS detection

Cells were collected at the end of fermentation from each run. The H_2O_2 content was calculated by measuring the absorbance at 390 nm. The cells were suspended in 3% trichloroacetic acid solution (2.5 mL), and centrifuged at 12000 × *g* and 4 °C for 10 min. Then 1 mL of the supernatant was mixed with equal volume of PBS buffer (pH 7), followed by adding 2 mL 1 mol/L potassium iodide. The cells were resuspended in PBS buffer (50 mM, pH 7.8) containing 1 mmol/L EDTA and 1% (v/v) PVP, sonicated and then centrifuged at 12000 × *g* and 4 °C for 10 min. The supernatant was used for $O_2^{\bullet-}$, superoxide dismutase (SOD) and catalase (CAT) analysis, and protein concentration in the supernatant was determined by the Bradford assay. The effect of constant methanol feeding rate on $O_2^{\bullet-}$ content was measured by determining nitrite production [24].

Determination of lipid peroxidation

Cells were collected at the end of fermentation from each run, washed with PBS buffer and suspended in the same buffer. Malondialdehyde (MDA) was quantified by measuring thiobarbituric acid reactive substances as described previously [25]. The cell suspension treated with snailase and digestion buffer (Sangon Biotech, shanghai, China) were centrifuged at 10,000 × *g* for 15 min at 4 °C. One volume of the supernatant was mixed with two volumes of TBA reactive (0.25 M chlorhydric acid, 15% (v/v) trichloroacetic acid and 0.375% (w/v) thiobarbituric acid). Subsequently, the samples were incubated for 20 min at 100 °C in a dry bath, and then the mixture was cooled on ice and centrifuged at 12,000 × *g* for 30 s at 4 °C. Supernatant absorbance was measured at 532 nm.

SOD, CAT, and GSH assays

Process cell samples according to section 2.6. SOD activity, CAT activity and reduced glutathione (GSH) content were determined by their cellular analysis kits, respectively (Nanjing Jiancheng BioENG, Co., Nanjing, China).

RNA isolation and quantitative real-time PCR (RT-qPCR)

Cells were collected at the time point corresponding to the maximum enzyme activities. Total yeast RNA was extracted using RNAiso Plus (Takara, Dalian, China) according to the manufacturer's instructions. The cDNA was synthesized using PrimeScript^{TM} RT reagent Kit with gDNA Eraser (Takara, Dalian, China). RT-qPCR was conducted in CFX96 Real-Time PCR Detection System (Bio-Rad, Hercules, CA), and SYBR Green PCR Master Mix kit (Takara, Dalian, China) was used for the real-time PCR analysis. The primers used for RT-qPCR are listed in Table 2. The relative expressions of target genes were calculated by the $2^{-\Delta\Delta Ct}$ method [26].

Statistical analysis

All data are presented as means ± SD. The statistical significance was determined using one-way analysis of variance (ANOVA). Comparisons between two groups were conducted using Student's *t* test. A value of $p < 0.05$ was regarded as significant different.

Results

Growth kinetics on methanol

The time course of total cell growth and the methanol level was controlled by the sensor. Exponential growth was observed within 144 h of methanol feeding time. Based on the obtained maximum growth rate ($\mu_{MeOH,m}$) and maximum methanol specific consumption rate ($v_{MeOH,m}$) in the induction phase, we conducted fed-batch fermentations with different desired growth rates, $\mu_{MeOH,d}$ ($\leq\mu_{MeOH,m}$), by feeding methanol at a feed rate, F_{MeOH}, estimated as in [27-30]:

$$F_{MeOH} = v_{MeOH} X_0 V_0 e^{\mu_{MeOH,dt}}$$
$$= \mu_{MeOH,d} v_{MeOH,m} X_0 V_0 e^{\mu_{MeOH,dt}/\mu_{MeOH,m}} \quad (1)$$

where X_0 and V_0 are the cell density and broth volume at the beginning of the methanol fed-batch phase, and t the feed time of methanol. An actual μ_{MeOH} and v_{MeOH} were obtained from each run, and the linear dependence of μ_{MeOH} on v_{MeOH} is shown in Fig. 1. The methanol v_{MeOH} was exponentially fed into the bioreactor to support μ_{MeOH} using Herbert-Pirt linear relationship:

$$v_{MeOH} = 0.7281\ \mu_{MeOH} + 0.0098 \quad (2)$$

According to Eqs. (1) and (2), in the fed-batch fermentation process, the average biomass yield and maintenance coefficient of *P. pastoris* were 1.37 (g WCW/g MeOH) and 0.0098 (g MeOH/g WCW/h), respectively. Equation (2) was substituted in to Eq. 1, to give Eq.3:

$$F_{MeOH} = (0.7281\ \mu_{MeOH} + 0.0098) X_0 V_0 e^{\mu_{MeOH,dt}} \quad (3)$$

Effect of specific growth rate on fermentation performance

Fig. 2 shows the time courses of WCW, lipase activity and total protein concentration throughout the production phase with different specific growth rates. The specific growth rate had a direct impact on the cell growth rate and biomass. Higher specific growth rate led to greater cell growth. At postinduction times of 150, 126, 126 and 102 h, the attainable cell densities for the four rates were 392, 436 and 448 and 479 g/L, respectively. During the first 24 h after induction, protein production and lipase activity was similar for the four rates. However, the maximum total protein concentration value and lipase activity reached were 2.78 mg/mL and 1166.5 U/mL for the specific growth rate of 0.05 1/h. Lipase MAS1 was found to have one N-glycosylation site by N-glycosylation site analysis, but SDS–PAGE showed that there was one form of recombinant protein with molecular masses about 29 kDa. The recombinant protein

accounted for approximately 90% of the total protein in the culture supernatant which was estimated by the software quantity one (Bio-Rad). *P. pastoris* secreted few native proteins which facilitate downstream processing (Fig. 2D). As shown in Table 2, when the specific growth rate increased in the range of 0.015 to 0.05 1/h, the average specific production rate increased significantly. Especially when the specific growth rate was 0.05 1/h, the average specific production rate reached 0.052 mg/g WCW/h.

Effect of specific growth rate on cell viability and cell death

Fig. 3A shows the effect of specific growth rate on cell viability in a 5-L bioreactor. At all four rates, the cell activity decreased with the extension of induction time. Among the 0.015, 0.035 and 0.05 1/h, the specific growth rate showed an apparent flow rate-dependent positive effect on *P. pastoris* cell viability. The cell viability decreased significantly after 72 hours of induction for rates of 0.015, 0.035 and 0.05 1/h. From the process point of 0.065 1/h, the transition of rapid decline in cell viability was advanced to 48 h after induction. Fig. 3B shows that each group of cells had different amounts of red fluorescence after staining with propidium iodide. Normal cells could not be stained, the early apoptotic cells showed weak red fluorescence, the late apoptotic cells showed enhanced red fluorescence, and the dead cells showed strong red fluorescence. The number of cells showing propidium iodide-positive (red fluorescence) was higher at 0.065 1/h, and the cells mainly showed weak fluorescence intensity. Moreover, the percentage of propidium iodide-positive cells in other feeding rates showed lower red fluorescence, and most cells exhibited enhanced red fluorescence. From the above results, the specific growth rate 0.05 1/h appears to be most preferable because it maintained the highest cell viability and the lowest level of cell death.

Effect of specific growth rate on lipid peroxidation and ROS accumulation

As shown in Fig. 4, four specific growth rates did not cause a significant increase in $O2^{\bullet-}$ content in *P. pastoris*. However, *P. pastoris* had higher cellular $O^{2\bullet-}$ levels with 0.065 1/h in the induction phase compared with that in other methanol feeding induction conditions. Moreover, higher specific growth rates resulted in increased cellular H_2O_2 levels. Notably, for specific growth rate 0.065 1/h, the cellular H_2O_2 levels were significantly higher than other induction groups. For example, the cellular H_2O_2 levels reached were 2.2 nmol/min/mg-WCW for specific growth rate of 0.065 1/h. However, the cellular H_2O_2 level being 1.0 nmol/min/mg-WCW at specific growth rate of 0.05 1/h. Compared to 0.035 1/h, the rate of 0.05 1/h yielded a slight increase in cellular H_2O_2 level. The MDA levels were determined in order to evaluate oxidative damage in the cell of recombinant *P. pastoris* exposed to four specific growth rates (Fig. 4). The MDA levels were similar for the specific growth rates of 0.015, 0.035 and 0.05 1/h at the end of fermentation. By contrast, 0.065 1/h at 96 h showed a significant higher MDA level with respect to the other induction groups.

Effect of specific growth rate on cellular ROS scavenging system

We assayed activities of SOD and CAT, and the content of reduced GSH. Except for the increase of CAT activity, the results showed that higher specific growth rates caused nearly no change of SOD activity, and an obvious decrease in concentration of GSH with the specific growth rate of 0.065 1/h (Table 3). Moreover, the CAT activity with a specific growth rate of 0.05 1/h showed no comparable difference with that 0.035 1/h, whereas the CAT activity in with the specific growth rate of 0.065 1/h increased obviously.

Correlation of fermentation performance with ROS-associated parameters

Fig. 5 gives the heatmap constructed by Spearman's correlation analysis, to explore the correlations of fermentation performance and with ROS-associated parameters. The relevant parameters causing the accumulation of ROS in *P. pastoris* cells were related to the specific growth rate. Generally, high cell biomass and higher cell viability were beneficial for increasing total protein content and lipase activity. However, cell viability was negatively correlated with the cell biomass. But higher cell viability is beneficial for increasing protein content and lipase activity. Also, those interventions were further regulated by GSH levels.

RT-qPCR analysis of intracellular gene expression

Fig. 6 shows that the ROS scavenging system-related gene was amplified from the cDNA, and all samples were compared with the specific growth rate 0.035 1/h. Fig. 6 shows that higher specific growth rates caused a down-regulation of glutathione peroxidise (GPX1) and glutathione reductase (GLR1) at the mRNA levels. CAT expression at the mRNA level was higher for rates of 0.05 and 0.065 1/h compared with that 0.035 1/h. Especially, specific growth rate 0.065 1/h had a significantly higher expression of CAT at the mRNA level compared with that specific growth rate 0.035 1/h ($p < 0.05$). Moreover, cSOD, GPX1 and GLR1 mRNA level was higher for rate of 0.05 1/h in the methanol induced phase than that 0.065 1/h.

Discussion

P. pastoris is extensively used to produce various heterologous proteins. Amounts of biopharmaceutical drugs and industrial enzymes have been successfully produced by fed-batch high-cell-density fermentation of this cell factory. Although high-density fermentation of *P. pastoris* is considered as a promising development, it also has its limitations. It is not reliable to judge methanol concentration by dissolved O_2 alone in the fermenter, because the accumulation of intracellular toxic byproducts from methanol oxidation may cause cytotoxic to cells. Therefore, it is necessary to seek more perfect methods to promote protein production based on reducing the accumulation of toxic by-products of methanol oxidation.

The specific growth rate had a direct impact on the cell growth rate and cell biomass. The specific growth rate 0.015 1/h gave the lowest cell biomass. Compared to 0.035 and 0.05 1/h, the specific growth rate 0.015 1/h yielded a lower total protein concentration and enzyme activity. These results indicated that lack of carbon/energy sources could not meet the sufficient requirements for the cell metabolism,

and could also cause declines in cellular metabolic activity. For this reason, while cell viability at the specific growth rate 0.015 1/h was still similar after 72 h of induction, but the final value after 144 h induction was lower than that of 0.035 and 0.05 1/h. By contrast, although the specific growth rate 0.065 1/h caused rapid accumulation of total protein concentration and enzyme activity during the first 96 h after induction. However, from the process of the induction phase, the 0.035 and 0.05 1/h, especially specific growth rate 0.05 1/h appears to be most preferable because it produced the highest total protein concentration and highest enzyme activity. Current research recognized that excessive methanol would damage the AOX1 transcriptional efficiency and cellular metabolic activity, particularly when cells are exposed to high methanol concentration for a long time, as excessive methanol and dissolved oxygen may lead to the accumulation of formaldehyde, the first intermediate of methanol metabolism, to certain toxic levels [31]. Our study showed that a higher specific growth rate (0.065 1/h) resulted in a rapid decrease in cell activity. One reason might be that higher methanol toxicity maintained low cell viability, which could help to cell lysis. The conclusions and results could be found in related reports [32]. However, we further investigated that the accumulation of ROS from methanol oxidation may cause oxidative damage to cells. Difference from the accumulation of formaldehyde to certain toxic levels, in this study, the decline in cell activity caused by oxidative damage was also considered as one of the crucial factors for the metabolic toxicity of methanol.

Accumulation of ROS in cells caused by methanol feeding can form oxidative damage. MDA is a by-product of lipid peroxidation and reflects the degree of oxidative damage caused by ROS. For the specific growth rate 0.065 1/h, the cellular ROS accumulation and MDA levels were significantly higher than other induction conditions, indicating that the higher specific growth rates led to a significant increase in lipid peroxidation in *P. pastoris*. Generally, the cellular ROS scavenging system attenuates the oxidative damage by scavenging ROS, but excessive H_2O_2, which is not scavenging in time, can damage the lipids on the cell membrane [33]. Since membrane phospholipids are rich in unsaturated fatty acids and the hydrophobic membrane has a high solubility for oxygen atoms, so it is most vulnerable to free radicals [34]. So here we indeed found that the oxidative damage induced by the accumulation of ROS at the specific growth rate 0.065 1/h can cause cell apoptosis at an early stage and reduced protein expression ability.

Therefore, controlling intracellular ROS accumulation is beneficial for improving protein production in *P. pastoris* during the methanol induction phase. Evidence from our study demonstrated that the specific growth rate 0.05 1/h can stabilize the ROS scavenging system. Notably, the ROS accumulation level that affects total protein concentration and enzyme activity was closely related to cell viability. Those interventions were further regulated by GSH levels. Other protein factors are also effective defense strategies to ameliorate the toxic effects of ROS, such as GPX1 and CAT. While GPX and CAT utilize H_2O_2 as substrate, GSH protects cells from oxidative stress and endogenous toxic metabolites through HCHO metabolism and detoxification of ROS [35]. Actually, GPX1 also acts as a prophylactic antioxidant enzyme, with GSH to attenuate ROS accumulation, and is converted from the oxidized (GSSG) to reduced form (GSH) by GLR1 [36]. In this study, instead of increase, the concentration of GSH decreased along

with ROS accumulation, suggesting higher specific growth rates induced damage to the cellar ROS scavenging system. Since GLR1 and GPX1 control the cycle of transition between GSH and GSSG, the significantly high expression levels of their encoding gene expressions indicate smoothness of the transformation, thus explaining the reason for the high GSH content at specific growth rates of 0.015 to 0.05 1/h. It was reported that *p*53 reactivation and induction of massive apoptosis (PRIMA-1Met) inducing myeloma cell death by impairing GSH/ROS balance in human myeloma cell lines [37]. Similarly, titanium dioxide nanoparticles might cause a PRIMA-1Met-like effect in *P. pastoris*, independent of titanium dioxide nanoparticles [38]. However, in this study, methanol acts as a carbon source and inducer for *P. pastoris*. We supposed that metabolic by-product (H_2O_2), methanol oxidation may cause the accumulation of ROS, and induce oxidative damage to cells via impairing ROS scavenging system, especially GSH system, thereby reducing protein expression ability.

Conclusions

Methanol-feeding as a crucial operating parameter increases heterologous protein productivity by *P. pastoris*, but the accumulation of intracellular toxic byproducts from methanol oxidation may cause oxidative damage to cells. Our study demonstrates that controlling the specific growth rate of 0.05 1/h promoted protein production by selectively balancing ROS scavenging system and reducing oxidative damage to cells. Importantly, specific growth rate within suitable range can maintained a high content of GSH. Our findings help understand methanol-induced intracellular bioreaction network in high-cell-density fermentation. This strategy may serve as reference for similar fermentation processes.

Abbreviations

ROS: Reactive oxygen species; WCD: Wet cell density; AOX: Alcohol oxidase; SOD: Superoxide dismutase; CAT: Catalase; GSH: Reduced glutathione; MDA: Malondialdehyde; cSOD: Cytosolic superoxide dismutase; mSOD: Mitochondrial superoxide dismutase; GPX: Glutathione peroxidise; GLR: Glutathione reductase; YPD: Yeast extract peptone dextrose; BSM: Basal salt medium; FLU: Fluorescence density; RFLU: Relative fluorescence density.

Declarations

Author Contribution Rongkang Hu and Yonghua Wang designed the study. Rongkang Hu did experimental work. Rongkang Hu, Ruiguo Cui and Yonghua Wang collected and analyzed the data. Rongkang Hu wrote the manuscript with support from Qingqing Xu, Dongming Lan, Liu Yang, Ruiguo Cui and Yonghua Wang. All the authors read and approved the manuscript for publication.

Funding This work was supported by the National Key R & D Program of China (2018YFC0311104), National Science Fund for Distinguished Young Scholars (31725022), Key Program of Natural Science Foundation of China (31930084), Guangdong marine economy promotion projects (MEPP) Fund (no. GDOE[2019]A20).

Data availability The data produced and/or analyzed in the current study are available from the corresponding author on reasonable request.

Code Availability Not applicable.

Declarations

Conflicts of interest The authors declare no competing financial interests.

Ethics Approval Not applicable.

Consent to Participate Not applicable.

Consent for Publication Not applicable.

References

1. Shang, T., Si, D., Zhang, D., Liu, X., Zhao, L., Hu, C., Fu, Y., & Zhang, R. (2014). Enhancement of thermoalkaliphilic xylanase production by *Pichia pastoris* through novel fed-batch strategy in high cell-density fermentation. *BMC Biotechnology*, *17*(1), 311-316.

2. Calik, P., Bayraktar, E., Inankur, B., Soyaslan, E. S., Sahin, M., Taspinar, H., & Ozdamar, T. H. (2010). Influence of pH on recombinant human growth hormone production by *Pichia pastoris*. *Journal of Chemical Technology and Biotechnology*, *85*(12), 1628-1635.

3. Wang, J., Wu, Z., Zhang, T., Wang, Y., & Yang, B. (2019). High-level expression of *Thermomyces dupontii* thermophilic lipase in *Pichia pastoris* via combined strategies. *3 Biotech*, *9*(2), 1-9.

4. Su, X., Geng, X., Fu, M., Wu, Y., Yin, L., Zhao, F., & Chen, W. (2017). High-level expression and purification of a Mollusca endoglucanase from *Ampullaria crossean* in *Pichia pastoris*. *Protein Expression & Purification*, *139*, 8-13.

5. Yu, Y., Zhou, X., Wu, S., Wei, T., & Yu, L. (2014). High-yield production of the human lysozyme by *Pichia pastoris* SMD1168 using response surface methodology and high-cell-density fermentation. *Electronic Journal of Biotechnology*, *17*(6), 311-316.

6. Zhang, W., Bevins, M. A., Plantz, B. A., Smith, L. A., & Meagher, M. M. (2000). Modeling *pichia pastoris* growth on methanol and optimizing the production of a recombinant protein, the heavy-chain fragment C of botulinum neurotoxin, serotype A. *Biotechnology and Bioengineering*, *70*(1), 1-8.

7. Kupcsulik, B., Sevella, B., Ballagi, A., & Kozma, J. (2001). Evaluation of three methanol feed strategies for recombinant *pichia pastoris* muts fermentation. *Acta Alimentaria*, *30*(1), 99-111.

8. Gao, M., Dong, S., Yu, R., Wu, J., Zheng, Z., Shi, Z., & Zhan, X. (2011). Improvement of ATP regeneration efficiency and operation stability in porcine interferon-α production by *Pichia pastoris* under lower

induction temperature. *Korean Journal of Chemical Engineering*, *28*(6), 1412-1419.

9. Gao, M., Li, Z., Yu, R., Wu, J., Zheng, Z., Shi, Z., Zhan, X., & Lin, C. (2012). Methanol/sorbitol co-feeding induction enhanced porcine interferon-α production by *P. pastoris* associated with energy metabolism shift. *Bioprocess and Biosystems Engineering*, *35*(7), 1125-1136.

10. Gellissen, G. (2000). Heterologous protein production in methylotrophic yeasts. *Applied Microbiology and Biotechnology*, *54*(6), 741-750.

11. Barrigón, J. M., Montesinos, J. L., & Valero, F. (2013). Searching the best operational strategies for *Rhizopus oryzae* lipase production in *Pichia pastoris* Mut^+ phenotype: Methanol limited or methanol non-limited fed-batch cultures? *Biochemical Engineering Journal*, *75*(1), 47-54.

12. Dan, W., Chu, J., Hao, Y., Wang, Y., Zhuang, Y., & Zhang, S. (2011). High efficient production of recombinant human consensus interferon mutant in high cell density culture of *Pichia pastoris* using two phases methanol control. *Process Biochemistry*, *46*(8), 1663-1669.

13. Landolfo, S., Politi, H., Angelozzi, D., & Mannazzu, I. (2008). ROS accumulation and oxidative damage to cell structures in *Saccharomyces cerevisiae* wine strains during fermentation of high-sugar-containing medium. *Biochimica et Biophysica Acta-General Subjects*, *1780*(6), 892-898.

14. Ribeiro, T. P., Fernandes, C., Melo, K. V., Ferreira, S. S., & Horn, A. (2015). Iron, copper, and manganese complexes with in vitro superoxide dismutase and/or catalase activities that keep *Saccharomyces cerevisiae* cells alive under severe oxidative stress. *Free Radical Biology and Medicine*, *80*, 67-76.

15. Qiu, Z., Liu, X., Tian, X., & Yue, M. (2008). Effects of CO_2 laser pretreatment on drought stress resistance in wheat. *Journal of Photochemistry and Photobiology B: Biology*, *90*(1), 17-25.

16. Vanz, A. L., Lünsdorf, H., Adnan, A., Nimtz, M., Gurramkonda, C., Khanna, N., & Rinas, U. (2012). Physiological response of *Pichia pastoris* GS115 to methanol-induced high level production of the Hepatitis B surface antigen: catabolic adaptation, stress responses, and autophagic processes. *Microbial Cell Factories*, *11*(1), 103-113.

17. Haynes, C. M., Titus, E. A., & Cooper, A. A. (2004). Degradation of misfolded proteins prevents er-derived oxidative stress and cell death. *Molecular Cell*, *15*(5), 767-776.

18. Schwarzhans, J., Luttermann, T., Geier, M., Kalinowski, J., & Friehs, K. (2017). Towards systems metabolic engineering in *Pichia pastoris*. *Biotechnology Advances: An International Review Journal*, *35*(6), 681-710.

19. Lan, D., Qu, M., Yang, B., & Wang, Y. (2016). Enhancing production of lipase MAS1 from marine *Streptomyces* sp. strain in *Pichia pastoris* by chaperones co-expression. *Electronic Journal of Biotechnology*, *22*(4), 62-67.

20. Yuan, D. Lan, D., Xin, R., Yang, B., & Wang, Y. (2016). Screening and characterization of a thermostable lipase from marine *Streptomyces* sp. strain W007. *Biotechnology & Applied Biochemistry*, *63*(1), 41-50.

21. Li, H., & Xia, Y. (2019). High-yield production of spider short-chain insecticidal neurotoxin Tx4(6–1) in *Pichia pastoris* and bioactivity assays in vivo. *Protein Expression and Purification*, *154*, 66-73.

22. Zhang, X., Ai, Y., Xu, Y., & Yu, X. (2019). High-level expression of *Aspergillus niger* lipase in *Pichia pastoris*: Characterization and gastric digestion in vitro. *Food chemistry*, *247*, 305-313.

23. Sinha, J., Plantz, B. A., Inan, M., & Meagher, M. M. (2010). Causes of proteolytic degradation of secreted recombinant proteins produced in methylotrophic yeast *Pichia pastoris*: case study with recombinant ovine interferon-tau. *Biotechnology and bioengineering*, *89*(1), 102-112.

24. Liu, T., Zhu, L., Wang, J., Wang, J., Zhang, J., Sun, X., & Zhang, C. (2015). Biochemical toxicity and DNA damage of imidazolium-based ionic liquid with different anions in soil on Vicia faba seedlings. *Scientific reports*, *5*(1), 18444-18453.

25. Zepeda, A. B., Figueroa, C. A., Pessoa, A., & Farías, J. G. (2018). Free fatty acids reduce metabolic stress and favor a stable production of heterologous proteins in *Pichia pastoris*. *Brazilian journal of microbiology*, *49*(4), 856-864.

26. Livak, K., & Schmittgen, T. (2000). Analysis of relative gene expression data using real-time quantitative PCR and the $2^{-\triangle\triangle Ct}$ method. *Methods*, *25*(4), 402-408.

27. Zhang, W. Potter, K. J. H., Plantz, B. A., Schlegel, V. L., Smith, L. A., & Meagher, M. M. (2003). *Pichia pastoris* fermentation with mixed-feeds of glycerol and methanol: growth kinetics and production improvement. *Journal of industrial microbiology & biotechnology*, *30*(4), 210-215.

28. Rebnegger, C., Vos, T., Graf, A. B., Valli, M., Pronk, J. T., Daran-Lapujade, P. A. S., & Mattanovicha, D. (2016). *Pichia Pastoris* exhibits high viability and a low maintenance energy requirement at near-zero specific growth rates. *Applied & Environmental Microbiology*, *82*(15), 4570-4583.

29. Sinha,
J., Plantz, B. A., Zhang, W., Gouthro, M., Schlegel, V., Liu, C. P., & Meagher, M. M. (2003). Improved production of recombinant ovine interferon-τ by Mut^+ strain of *Pichia pastoris* using an optimized methanol feed profile. *Biotechnology Progress*, *19*(3), 794-802.

30. Rahimi, A., Hosseini, S. N., Jauidanbardan, A., & Khatami, M. (2019). Continuous fermentation of recombinant *Pichia pastoris* Mut(+) producing HBsAg: Optimizing dilution rate and determining strain-specific parameters. *Food & Bioproducts Processing*, *118*(part C), 248-257.

31. Wu, D., Zhu, H., Chu, J., & Wu, J. (2019). N-acetyltransferase co-expression increases α-glucosidase expression level in *Pichia pastoris*. *Journal of biotechnology*, *289*, 26-30.

32. Lee, J., Won, Y., Park, K., Lee, M., Tachibana, H., Yamada, K., & Seo, K. (2012). Celastrol inhibits growth and induces apoptotic cell death in melanoma cells via the activation ROS-dependent mitochondrial pathway and the suppression of PI3K/AKT signaling. *Apoptosis, 17*(12), 1275-1286.

33. Costa, V. M. V., Amorim, M. A., Quintanilha, A., & Moradas-Ferreira, P. (2002). Hydrogen peroxide-induced carbonylation of key metabolic enzymes in *Saccharomyces cerevisiae*: the involvement of the oxidative stress response regulators Yap1 and Skn7. *Free Radical Biology and Medicine*, *33*(11), 1507-1515.

34. Halliwell, B., & Gutteridge, J. M. C. (1985). Free radicals in biology and medicine. Fifth edn. Oxford, United Kingdom: Oxford University Press.

35. Fahey, C. R. (2001). Novel Thiols of Prokaryotes. *Annual Review of Microbiology*, *55*, 333-356.

36. Delic, M., Rebnegger, C., Wanka, F., Puxbaum, V., Haberhauer-Troyer, C., Hann, S., Kollensperger, G., Mattanovich, D., & Gasser, B. (2012). Oxidative protein folding and unfolded protein response elicit differing redox regulation in endoplasmic reticulum and cytosol of yeast. *Free Radical Biology and Medicine*, *52*(9), 2000-2012.

37. Tessoulin, B., Descamps, G., Moreau, P., Maiga, S., Lode, L., Godon, C., Marionneau-Lambot, S., Oullier, T., Le, G. S., Amiot, M., & Pellat-Deceunynck, C. (2014). PRIMA-1Met induces myeloma cell death independent of p53 by impairing the GSH/ROS balance. *Blood*. *124*(10), 1626-1636.

38. Liu, Z., Zhang, M., Han, X., Xu, H., Zhang, B., Yu, Q., & Li, M. (2016). TiO_2 nanoparticles cause cell damage independent of apoptosis and autophagy by impairing the ROS-scavenging system in *Pichia pastoris*. *Chemico-Biological Interactions*, *252*, 9-18.

Tables

Table 1 List of primers used to amplify mRNA by quantitative qRT-PCR

Gene	Forward primer (5′-3′)	Reverse primer (5′-3′)
Actin	GTCCAGCATAAACACGCCG	CAGTGGGAAAAACCCACGAA
cSOD	CGAACAATCCTCCGAAAG	ACCCTTGGCAACACCTTCA
CAT	GCTACTAACCTGAAGGACGC	TTGAAGTTTACGACACCCAG
GPX1	CCCATTAGATAAGAAAGGCG	CCAAACTGGTTACAGGGAA
GLR1	AACTTCGCCCAACCGTAT	TCTCAATCGCCAAGGACT
PDI1	GAACTTGTTTCTGCTGCCG	CAATGCTTTGGCTCTGTCTT
KAR2	AAGTCGGGTCGTGTAGAAAT	CGCTTCAAGTCTCTTTGGA
CCH1	TCAGAAACAAATCAGCCCG	AGTGGGCATTGTCCTTGAC
CRZ1	CTTCCTCCAAACGCTTCTTT	GTATTGGTTGAAGTCTTGGGC

Table 2 Effect of specific growth rate on MAS1 production

Specific growth rate (1/h)	Harvest time after induction (h)	Cell density (g WCW/L)	Volumetric MAS1 production (g/L)	Specific MAS1 production (mg/g WCW)	Average specific production rate (mg/g WCW/h)
0.015	144	384±6	1.8±0.08	4.69	0.033
0.035	120	424±10	2.39±0.12	5.64	0.047
0.05	120	444±16	2.78±0.08	6.26	0.052
0.065	96	465±16	2.21±0.09	4.75	0.049

Data are mean ± standard deviation of results from independent duplicate fermentations.

Table 3 Cellular ROS scavenging system in MAS1 fermentation by *Pichia pastoris* under different induction strategies

Specific growth rate (1/h)	SOD (U/mg-protein)	CAT (U/mg-protein)	GSH (mg/g-WCD)
0.015	1.8 ± 0.2	1.1 ± 0.1	1.5 ± 0.2
0.035	1.7 ± 0.1	1.6 ± 0.2	3.2 ± 0.3
0.05	1.9 ± 0.2	1.8 ± 0.1	3.0 ± 0.3
0.065	2.0 ± 0.1	2.7 ± 0.3	0.8 ± 0.2

Data are mean ± standard deviation of results from independent duplicate fermentations.

Figures

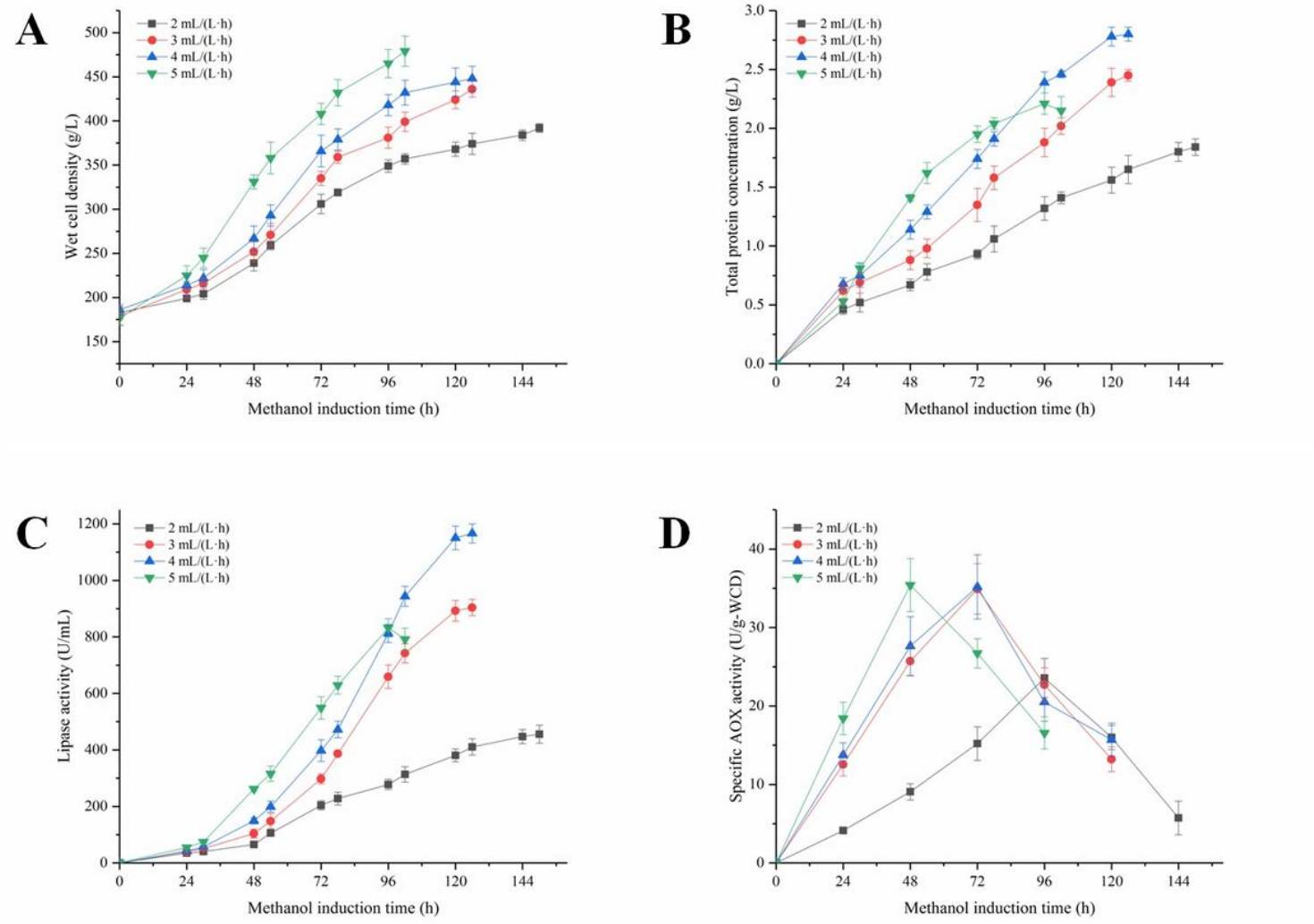

Figure 1

The relationship between methanol specific consumption rate and specific growth rate in fed-batch fermentation process recombinant P. pastoris expressing lipase MAS1.

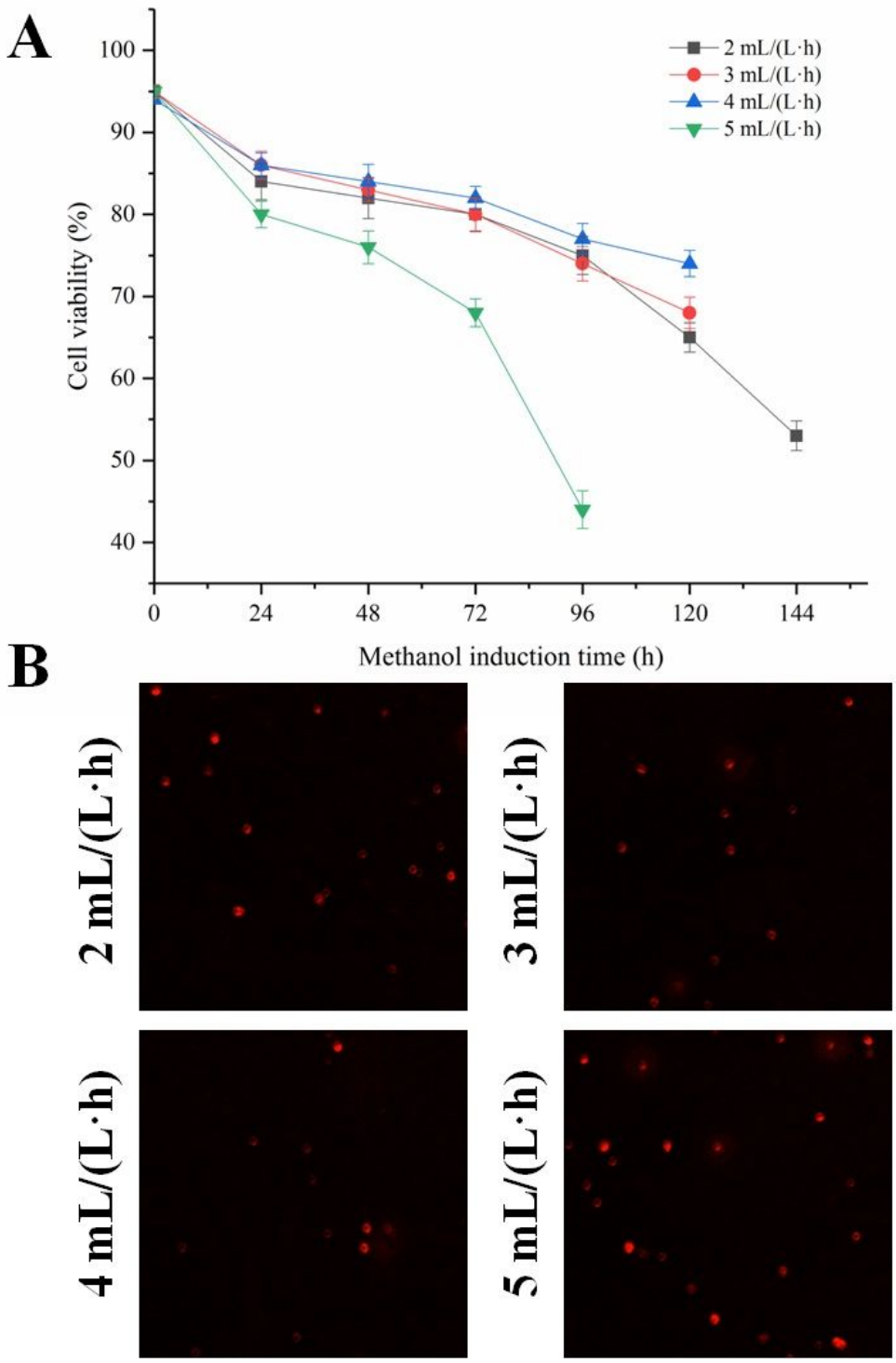

Figure 2

Effect of specific growth rate on the fermentation performance within the induction time. (A) wet cell weight (WCW), (B) lipase activity, (C) total protein concerntration and (D) SDS-PAGE analyses of culture supernatant at different specific growth rates. Lane 1, represented supernatant from initial fermentation; Lane 2-7, represented supernatant from 0 to120 h after induction at specific growth rate of 0.05 1/h. The error bars represent the results of the triplicate runs.

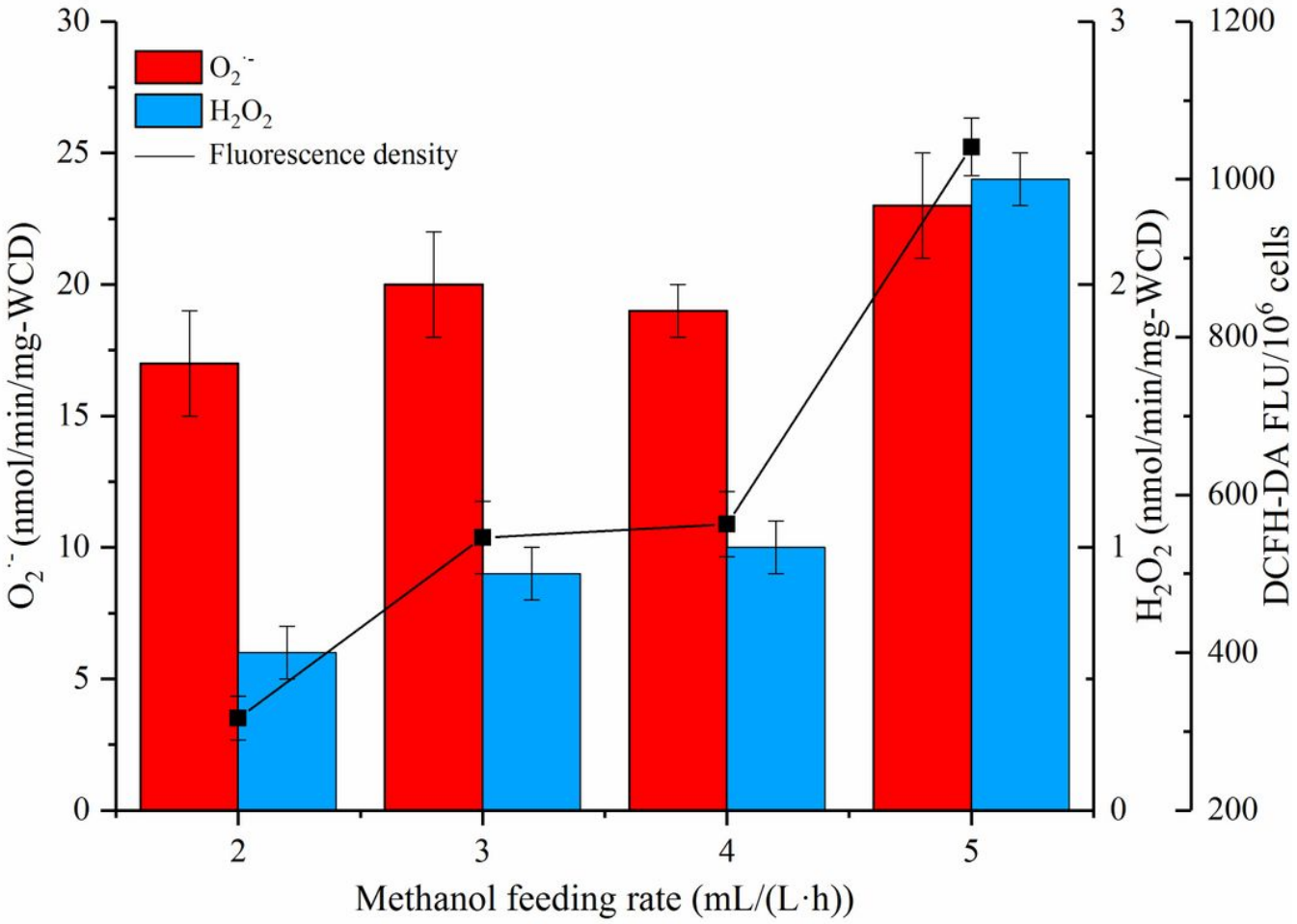

Figure 3

Effect of specific growth rate on cell viability and cell death. (A) Cell viability, and (B) cell death. The treated cells were stained with PI and observed by fluorescence microscopy. The percentage of propidium iodide-positive cells was calculated by the number of propidium iodide-positive cells divided by that of total cells×100. Error bars are the SD value calculated from triple experiments.

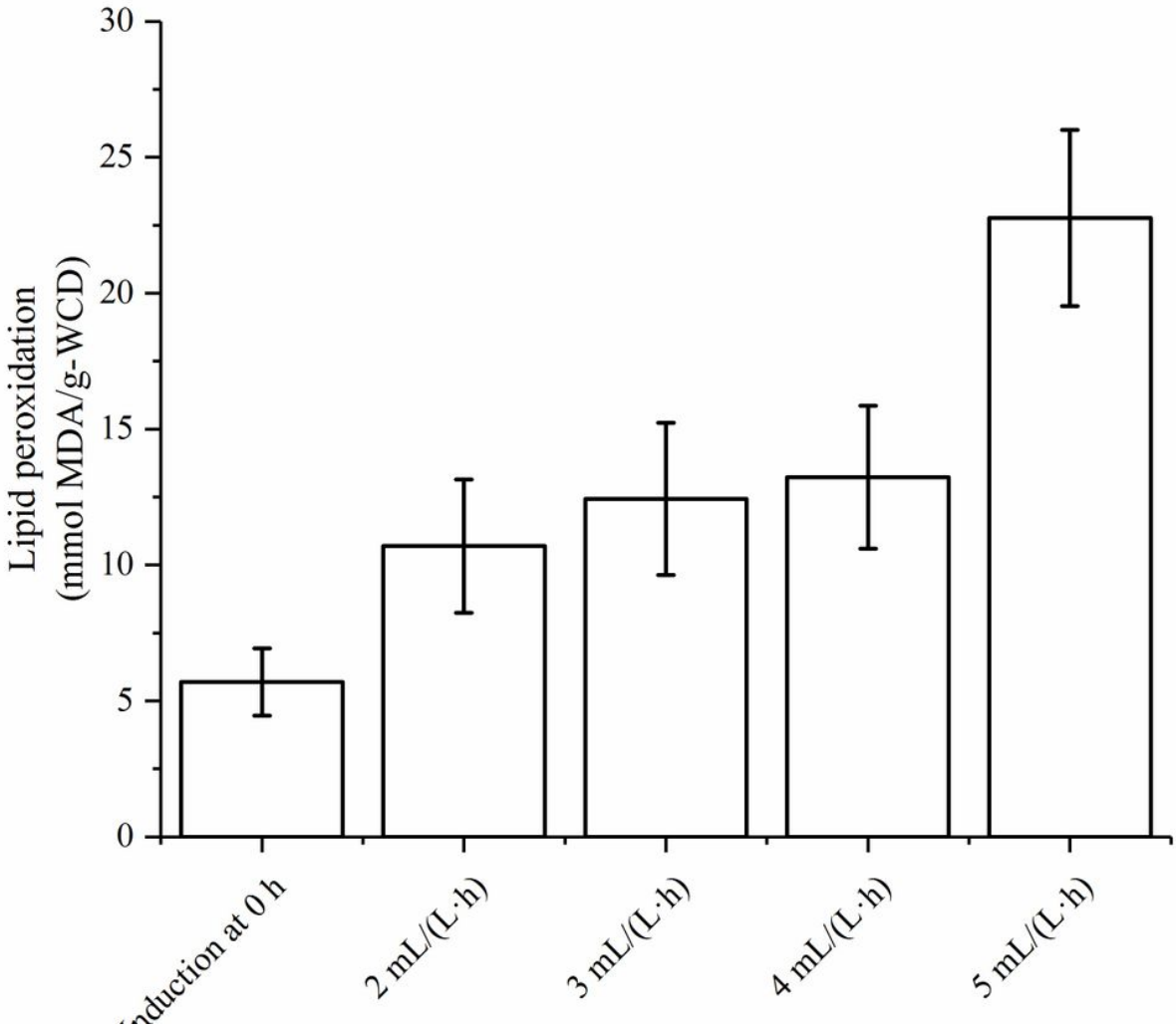

Figure 4

Effect of specific growth rate on reactive oxygen species (ROS) accumulation and lipid peroxidation (MDA). Error bars are the SD value calculated from triple experiments.

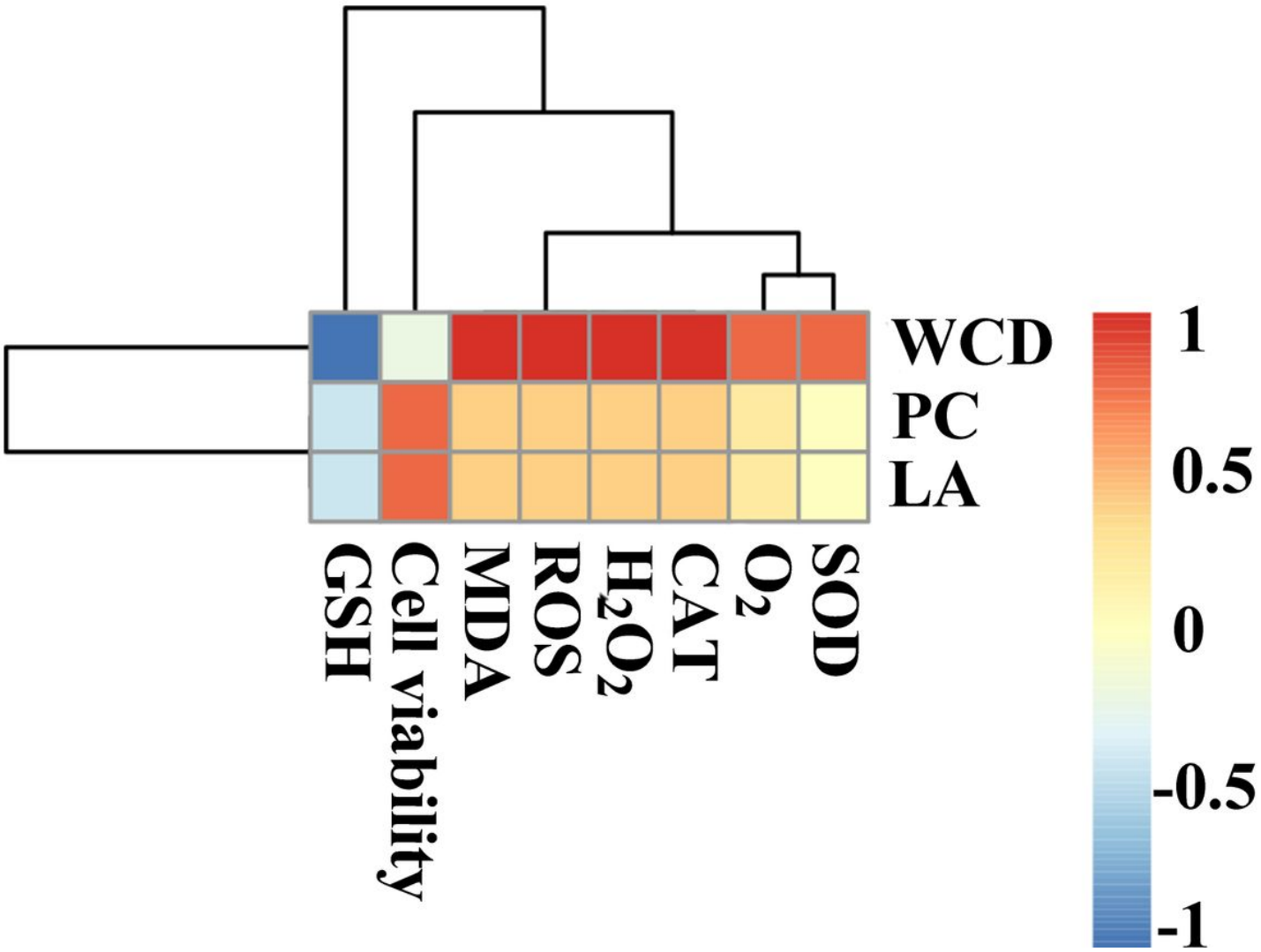

Figure 5

A Spearman's correlation heatmap was used to represent significant statistical correlation values (r) between fermentation performance and ROS-associated parameters with different methanol feeding rate. The intensity of the colour represents the degree of association between fermentation performance and ROS-associated parameters [numerical values: WCD: Wet cell density; PC: Total protein concentration; LA: Lipase activity].

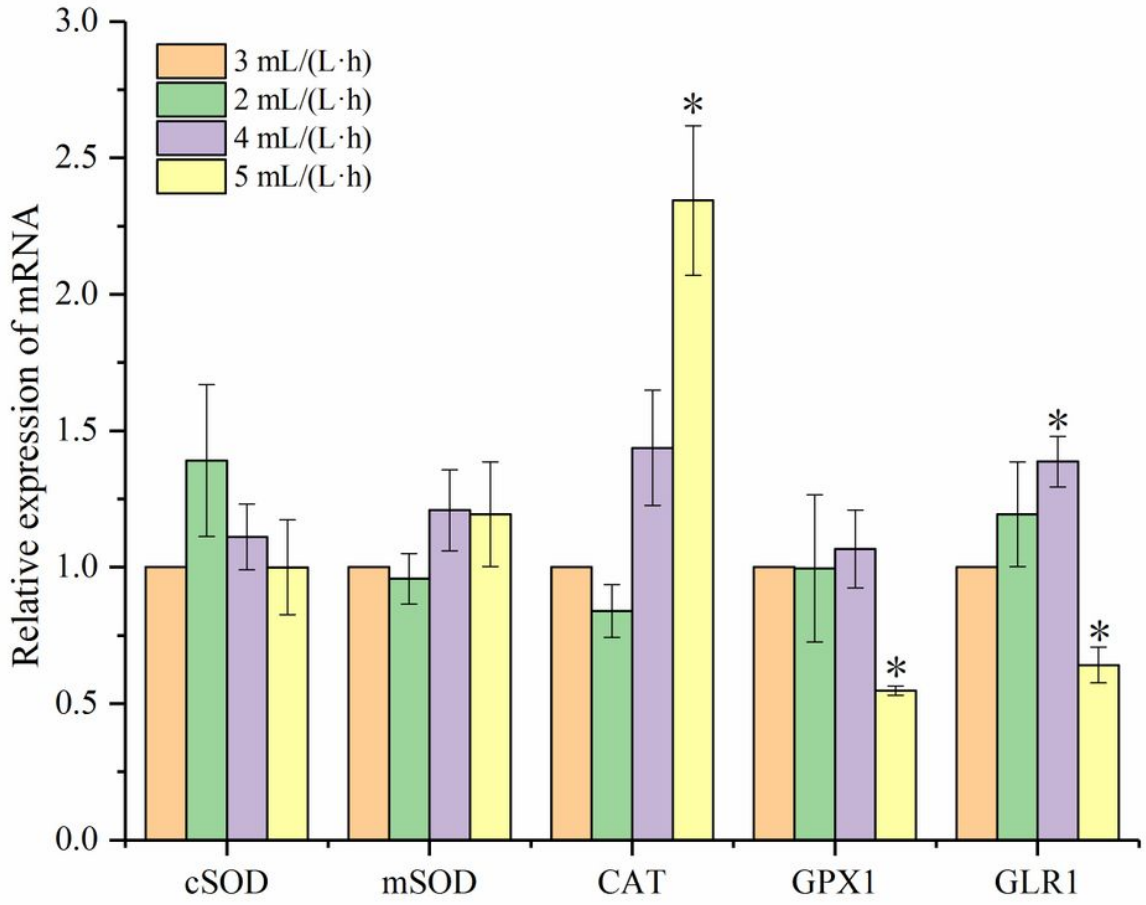

Figure 6

The expressions of genes at the mRNA levels were determined using RT-qPCR. Data were expressed as means ± SD. Differences were assessed by ANOVA and denoted as follows: *p < 0.05 versus specific growth rate 0.01 h-1.